

BATTERY VALUATION ON ELECTRICITY INTRADAY MARKETS WITH LIQUIDITY COSTS

ENZO COGNÉVILLE, THOMAS DESCHATRE, AND XAVIER WARIN

ABSTRACT. We propose a complete modeling framework to value several batteries in the electricity intraday market at the trading session scale. The model consists of a stochastic model for the 24 mid-prices (one price per delivery hour) combined with a deterministic model for the liquidity costs (representing the cost of going deeper in the order book). A stochastic optimization framework based on dynamic programming is used to calculate the value of the batteries. We conduct a backtest for the years 2021 to 2023 for the German and French markets. We show that accounting for liquidity is essential, especially when the number of batteries is large: it leads to significantly higher profits and prevents substantial losses under our liquidity model. The use of our stochastic model for the mid-price also improves the results (compared to a deterministic framework where the mid-price forecast is the spot price).

Keywords: Electricity intraday prices; Liquidity costs; Storage valuation; Dynamic programming.

Enzo Cogneville, EDF Lab Paris-Saclay and FiMe, Laboratoire de Finance des Marchés de l’Energie, 91120 Palaiseau, France.

Email adress: enzo.cogneville@edf.fr.

Thomas Deschatre, EDF Lab Paris-Saclay and FiMe, Laboratoire de Finance des Marchés de l’Energie, 91120 Palaiseau, France.

Email adress: thomas-t.deschatre@edf.fr.

Xavier Warin, EDF Lab Paris-Saclay and FiMe, Laboratoire de Finance des Marchés de l’Energie, 91120 Palaiseau, France.

Email adress: xavier.warin@edf.fr.

1. INTRODUCTION

1.1. Motivation. The capacity and production of renewable electricity are increasing every year; in France, for example, the aim is to achieve a 33% share of renewable energy in electricity consumption in 2030¹. However, the producers involved have to deal with the intermittent nature of these production resources, which are subject to the uncertainties of the weather and to outages of conventional thermal power plants. In Western Europe, in the spot market, producers submit their hourly production offers for the following day by noon on the day prior. They commit to delivering this production the next day at a predetermined price, known as the spot price, which is set for each hour. This balance is therefore based on a day-ahead production forecast, and this forecast can change. Producers can use the intraday electricity market to rebalance their positions, which opens at 3 p.m. (CET) the day before delivery and consists of one product for each hour of delivery, which can be bought or sold up to 5 to 30 minutes (depending on the country) before the hour of delivery. For more details on how the intraday market works, we refer the reader to [22, Section 2]. Another way of coping with this intermittency is to use storage resources such as batteries: the operator can then release energy from storage if there is a shortfall in production and store it otherwise. Batteries can also be used to respond to peaks in demand (or falls in production) by releasing energy from storage, or to very low demand (or excessively high production) by storing energy. To quantify the profitability of the battery, it is necessary to quantify the flexibility of this means of storage on the markets, in this case on the intraday market. Much theoretical work has been devoted to storage valuation [31, 9, 3] for example, see also [28] for a review, with the most recent being the work of Abi Jaber et al. [23] which includes market effects and transaction costs. On the empirical side, Deschatre and Warin [14] as well as Collet et al. [12] use dynamic programming to value a battery on the electricity intraday market (in [12], the battery is managed with a wind generation facility); Jiang and Powell [24] consider the real time market (hour-ahead) in the United States.

In [14, 12, 24], liquidity costs are not taken into account. These can have a significant impact, especially when a player uses several batteries simultaneously. In addition, the intraday market can have very high bid-ask spreads, which is a very important indicator of the cost of liquidity, see [4, 5]. Neglecting these costs can lead to an overestimation of battery yields and suboptimal investment decisions. Few papers have focused on modeling liquidity in intraday electricity markets. Favetto [15] models transaction price arrivals with a Hawkes process with time-dependent intensity. Graf von Luckner and Kiesel [20] consider the arrivals of market orders in the intraday order book and use a bivariate Hawkes process to model these arrivals; the evolution of this model's parameters is studied in [7]. In [26], Kramer and Kiesel extend the model of Graf von Luckner and Kiesel [20] by including exogenous factors such as forecasting errors in renewable energy production. They also consider limit and cancel orders independently. While all of these models provide insights into the behavior of liquidity in the intraday electricity market, they do not allow for the simulation of trading strategies or backtesting, which requires the simulation of the entire order book (or at least the mid-price with liquidity costs). Recently, Bergault and Cognéville [5] have proposed an order book modeling framework for illiquid markets, which is applied to French and German intraday electricity markets and can then be used to simulate trading strategies or asset pricing under liquidity costs. Bergault et Cognéville [5] (as well as all previously cited liquidity models) only consider a model for a given maturity and do not model the dependence between different order books, which is essential for the valuation of a storage asset. Glas et al. [19] study the limit order book and model the cost of executing a market order as a linear function of volume

¹<https://www.ecologie.gouv.fr>

with time-dependent parameters. They use their model to optimize the revenue of a portfolio of conventional and wind generation sold on the intraday electricity market. Kath and Ziel [25] follow the same approach using generalized additive models [33] to model the execution cost of a market order and solve the optimal execution problem.

1.2. Contribution. Our approach follows that of Glas et al. [19] and Kath and Ziel [25] and differs from that of Bergault and Cognéville [5]. For our case, modeling the entire order book across all 24 maturities of the EPEX market would result in an excessively high-dimensional framework, with 6 processes required for each maturity. Instead, we propose a model for mid-prices and a model for liquidity costs. This approach was first proposed for equity markets by Cetin et al. in [10] and Blais and Protter in [6]. They consider a share price per unit of volume that a trader pays (receives) when buying (selling) x units of the share in the market at time t (where $x > 0$ corresponds to a buy and $x < 0$ to a sell). The total price paid by the trader is then $xS(t, x)$ (which is negative when the trader receives money). Cetin et al. [10] consider the multiplicative model $S(t, x) = S(t, 0)e^{\alpha x}$, and the function $x \rightarrow e^{\alpha x}$ represents the supply curve corresponding to the cost of liquidity: the more you buy, the deeper you have to go in the order book and the more you pay per unit of volume. $S(t, 0)$ follows a Black-Scholes dynamic. Blais and Protter [6] consider an additive model of the form:

$$(1) \quad S(t, x) = S(t, 0) + M(t)x$$

and, for illiquid assets, an asymmetric model :

$$(2) \quad S(t, x) = (b_-(t) + M_-(t)x)\mathbf{1}_{x < 0} + (b_+(t) + M_+(t)x)\mathbf{1}_{x > 0}.$$

The parameters of the liquidity curve in [6] are estimated using the limit order book.

In this paper, we propose a model of both price and liquidity for intraday electricity prices that allows for the pricing of assets such as storage, whose value depends on the dynamics of prices for different maturities. We first perform an empirical analysis using limit order book data from EPEX for each maturity and analyze the liquidity curve (defined around the mid-price as in [29]). We fit a model close to (2) for the liquidity curve, which is more appropriate than (1) and shows evidence of market illiquidity. Our model takes into account some peculiarities of the intraday electricity markets, such as the increase in liquidity as the maturity approaches (Samuelson effect) [4]. These results are given in Section 2.1. For the dynamics of mid-prices, we consider the multivariate model of Deschatre and Warin [14], which has already been used for transaction prices and allows us to model several stylized facts observed for intraday electricity prices: volatility increases as maturity approaches, while correlation decreases with the distance between maturities, see Section 2.2. We provide orders of magnitude for the different parameters of the models (liquidity model and mid-price model), which may prove useful for researchers and practitioners. These parameters can be used, for example, to study optimal trading strategies or equilibrium pricing [2, 16, 1], which require volatility parameters for the price and transaction costs. An alternative to the Deschatre and Warin model [14] for mid-price simulation would be the model of Hirsch and Ziel [22] used for probabilistic forecasting, but it requires extensive input data, such as wind power forecasts.

To assess the quality of the liquidity model, the valuation of a storage asset, here a battery, in Section 3. We perform a backtest on real data for the French and German electricity intraday markets and compare the revenues obtained by optimizing the storage asset using our liquidity model and without a liquidity model. Applying the optimal controls obtained with a dynamic programming algorithm on real data, we show that revenues are higher when using a control that accounts for liquidity. Neglecting those costs can lead to substantial losses when a large number

of batteries is considered. It is therefore essential to include a liquidity model in the optimization process. We also show that the use of the stochastic model improves the value of the battery.

1.3. Dataset. The dataset consists of all orders submitted during each trading session in 2021, 2022, and 2023 on the French and German intraday electricity markets, provided by the market platform EPEX. For each delivery date, we have access to orders from 24 trading sessions covering the 24 delivery hours (or maturities, or products) of the day (we do not consider products with half-hourly or quarter-hourly delivery). These sessions start at 3 p.m. (CET) the day before delivery and end 5 minutes before the delivery hour (the trading duration therefore differs across maturities). For a given maturity, we have access to all limit and market orders sent to the market. Each order is marked with its creation time (to the millisecond), price, volume, and side (buy or sell). If the order is canceled at any time during the trading session, the cancellation date is recorded, which allows us to reconstruct canceled orders. Some orders may include trading restrictions, which we take into account: Immediate or Cancel (any part of the order not filled immediately is canceled), Fill or Kill (executed immediately at a specified price or canceled if not filled in full), All or None (the order is filled in full or canceled). In addition, some orders can be hibernated, i.e. deactivated and then reactivated, and some orders are block orders and link different markets. A block order is an order placed simultaneously on several products, the volume of which can only be executed on all products at once; block orders can only be matched with other block orders. Block orders are excluded from our analysis. Cross-border trading is possible through the Cross-Border Intraday (XBID) initiative, which allows order books to be aggregated across interconnected countries in Europe as long as the interconnections are not saturated. The last hour of trading before delivery is a specific period. First, cross-border transactions via the XBID mechanism are no longer possible from one hour before delivery, which significantly reduces liquidity since the order book is no longer coupled at the European level. Secondly, from one hour before delivery in France and 30 minutes in Germany², market participants can no longer modify their schedules submitted to the transmission system operator and therefore use the intraday market only to adjust residual imbalances. This also reduces market liquidity, as trading strategies become more constrained. Moreover, activating a battery during this period, if not properly anticipated and scheduled, may create an imbalance position. For these reasons, the last hour prior to delivery is excluded from the scope of this study, both in terms of data analysis and trading strategy modeling. The tick size is 0.01€/MWh. The reader can refer to [21, Appendix A] for a more detailed description of the data.

The limit order book is reconstructed from these orders using methods close to the ones described in [21, Section 3]: it consists of a snapshot at each point in time of the different buy and sell orders in the market, with their associated price and volume. Note that the limit order book reconstruction may not be exact for some trading sessions as some information is missing, especially on hibernated orders; see also [21, 17] which highlights issues related to the reconstruction. We retain the 20 best bid and ask quotes for France and the 60 best bid and ask quotes for Germany at each point in time during the trading session, which is sufficient for this work. For most traded products, the dataset contains fewer than 20 bid and ask quotes for the French market and fewer than 60 for the German market.

2. MODELING FRAMEWORK

Let $0 < T_1 < T_2 < \dots < T_M = T$ be the different maturities, with $M \in \mathbb{N} \setminus \{0\}$. We denote by $S_{m,t}(x)$ the price per unit of volume that a trader pays / receives when he buys / sells at date

²In Germany, between one hour and 30 minutes before delivery, trades can still occur between the four balancing zones.

t , x MWh of electricity (where $x > 0$ corresponds to a purchase and $x < 0$ to a sale) delivered at maturity T_m , the total price paid by the trader being $xS_{m,t}(x)$. This price is decomposed into the sum of two components:

- the mid-price, denoted by $f_{m,t}$, which is modeled by a stochastic process in Section 2.2,
- and the cost of liquidity, $L_m(t, x)$, modeled by a deterministic curve in Section 2.1.

2.1. Liquidity costs modeling. To capture liquidity costs in €/MWh, we use a linear jump model inspired by the framework developed by Blais and Protter [6] who generalized the linear model used by [19] for intraday electricity prices. The model is expressed as a function of time $0 \leq t \leq T_m$ and traded volume x :

$$(3) \quad L_m(t, x) = [A_{m,-}(t)x - B_{m,-}(t)]\mathbf{1}_{\{x < 0\}} + [A_{m,+}(t)x + B_{m,+}(t)]\mathbf{1}_{\{0 < x\}}, \quad t \leq T_m$$

where

- $A_{m,-}(t)$ and $A_{m,+}(t)$ are linear functions of the time to maturity $T_m - t$,

$$(4) \quad A_{m,\pm}(t) = \alpha_{A_{m,\pm}}(T_m - t) + \beta_{A_{m,\pm}},$$

- and $B_{m,-}(t)$ and $B_{m,+}(t)$ are exponential functions,

$$(5) \quad B_{m,\pm}(t) = e^{\alpha_{B_{m,\pm}}(T_m - t) + \beta_{B_{m,\pm}}}.$$

For a fixed time $0 \leq t \leq T_m$, the function $x \mapsto L_m(t, x)$ is piecewise linear in x , with different slopes for $x < 0$ (bid side) and $x > 0$ (ask side). The price per unit of volume due to liquidity costs increases linearly with volume, corresponding to a quadratic increase in total cost with volume. As time t approaches maturity T_m , we expect the slopes of $L_m(t, x)$, namely $A_{m,+}(t)$ and $A_{m,-}(t)$, to decrease as liquidity increases, corresponding to $\alpha_{A_{m,\pm}} > 0$. $B_{m,+}(t)$ and $B_{m,-}(t)$ encode the bid-ask spread, which is equal to $B_{m,+}(t) + B_{m,-}(t)$ and decreases as t approaches maturity T_m if $\alpha_{B_{m,\pm}} > 0$.

At time $t \in [0, T_m]$, for $i \geq 1$, let $V_{m,-i}(t) < 0$ denote the negative of the volume associated with the i^{th} best bid price $P_{m,-i}(t)$ and let $V_{m,i}(t) > 0$ denote the volume associated with the i^{th} best ask price $P_{m,i}(t)$ for maturity T_m . We then have $P_{m,i}(t) < P_{m,j}(t)$ if $i < j$. For $i \geq 1$, we denote by $\bar{V}_{m,-i}(t) = \sum_{k=1}^i V_{m,-k}(t)$ the cumulative bid volume at level i , and by $\bar{V}_{m,i}(t) = \sum_{k=1}^i V_{m,k}(t)$ the cumulative ask volume at level i . We also use the notation $V_{m,0}(t) = 0$ and $\bar{V}_{m,0}(t) = 0$. See Figure 1 for an illustration of the order book notation.

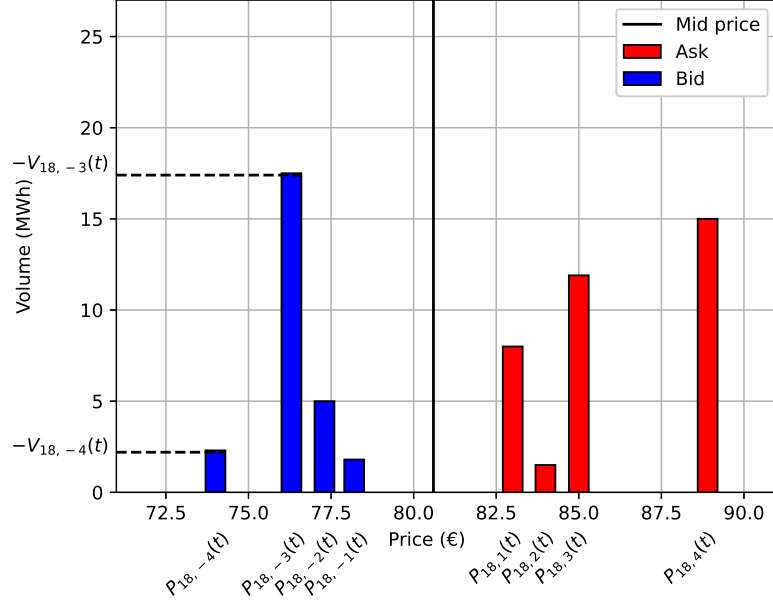


FIGURE 1. Order book illustration from [5].

First, in Figure 2, to justify a piecewise linear modeling for $x \mapsto L_m(t, x)$, we plot at fixed time $0 \leq t \leq T_m$ the average weighted prices at level i of the order book, $\frac{\sum_{k=1}^i P_{m,k}(t)V_{m,k}(t)}{V_{m,i}(t)}$ for the ask side and $\frac{\sum_{k=1}^i P_{m,-k}(t)V_{m,-k}(t)}{V_{m,-i}(t)}$ for the bid side against the cumulated volume $\bar{V}_{m,-i}(t)$ for the bid side and $\bar{V}_{m,i}(t)$ for the ask side. We employ the linear jump model (3) to analyze trading volumes within the ranges of $[-K, K] = [-20, 20]$ MWh for the French market and $[-100, 100]$ MWh for the German market: for bid and ask sides separately, we perform a linear regression of the weighted average price minus the mid-price

$$(6) \quad \begin{cases} p_{m,i}(t) = \frac{\sum_{k=1}^i P_{m,k}(t)V_{m,k}(t)}{V_{m,i}(t)} - \frac{P_{m,-1}(t)+P_{m,1}(t)}{2} & (\text{ask}) \\ p_{m,-i}(t) = \frac{\sum_{k=1}^i P_{m,-k}(t)V_{m,-k}(t)}{V_{m,-i}(t)} - \frac{P_{m,-1}(t)+P_{m,1}(t)}{2} & (\text{bid}) \end{cases}$$

at level $i \geq 1$ against the cumulated volume at the same level. These volume intervals $[-K, K]$ are determined empirically to ensure the validity of the linear approximation, as illustrated in Figure 2. Consequently, the battery valuation in Section 3 is restricted to these trading volumes. To model prices deeper in the order book, higher order polynomials or non-parametric functions may be used, as in [25]. For this reason, we focus on these volumes and estimate the parameters of the linear jump model accordingly. The estimated slopes of the order book curves fluctuate over time, and rare but significant shape shifts are observed during periods of market stress. The theory proposed by Blais and Protter [6] suggests that supply curves tend towards linearity near the end of a trading session due to increasing liquidity. However, this is not fully consistent with our observations. This discrepancy likely stems from persistent illiquidity toward the end of the session and from our consideration of deeper layers of the limit order book than Blais and Protter [6]. Finally, in practical optimization settings, a purely linear model may lead to suboptimal trading

decisions because it neglects bid-ask spread. One possible solution is to constrain the algorithm to avoid trading within the spread. The approach adopted here instead consists in constructing a liquidity cost model that distinguishes between buy and sell sides while maintaining a common spread parameter, thereby allowing appropriate trading bounds for each side.

In the following, we estimate the parameters of the model (3)-(4)-(5). The empirical liquidity cost curve minus the mid-price, which is the empirical counterpart of $L_m(t, x)$, can be exactly computed for any x within the range covered by the order book. It is piecewise concave, with breakpoints at each $\bar{V}_{m,\pm i}(t)$, where it takes the value $p_{m,\pm i}(t)$ (see the green solid curve in Figure 3). Several sampling schemes can be used to fit a linear model to this curve at a fixed time $0 \leq t \leq T_m$:

- (i) A first approach consists in considering the points on the empirical liquidity cost curve $(\bar{V}_{m,i}(t), p_{m,i}(t))$ for $i \neq 0$. The straight line passing through two successive points $(\bar{V}_{m,i}(t), p_{m,i}(t))$ and $(\bar{V}_{m,i+1}(t), p_{m,i+1}(t))$ lies below the empirical liquidity curve (minus the mid-price), since the latter is concave between these points. This leads to an underestimation of liquidity costs (see the blue curve *right regression* in Figure 3).
- (ii) To avoid underestimation, one may instead consider the upper bound of the empirical liquidity cost curve, defined as the piecewise constant function equal to $p_{m,i}(t)$:
 - on $]\bar{V}_{m,i-1}(t), \bar{V}_{m,i}(t)[$ for $i > 0$,
 - on $[\bar{V}_{m,i}(t), \bar{V}_{m,i+1}(t)[$ for $i < 0$
 (see the red curve *step evolution* in Figure 3). Sampling this upper bound at the rupture points, that is to consider the points $(\bar{V}_{m,i-1}(t), p_{m,i}(t))$ for $i > 0$ and $(\bar{V}_{m,i+1}(t), p_{m,i}(t))$ for $i < 0$, leads to an overestimation: the linear interpolation between two successive sampled points lies above both the upper bound and the true liquidity cost curve (see the orange curve *left regression* in Figure 3).
- (iii) Our empirical choice is a compromise between (i) and (ii). We consider the points
 - $(\frac{\bar{V}_{m,i-1}(t) + \bar{V}_{m,i}(t)}{2}, p_{m,i}(t))$ for $i > 0$,
 - and $(\frac{\bar{V}_{m,i}(t) + \bar{V}_{m,i+1}(t)}{2}, p_{m,i}(t))$ for $i < 0$.

This corresponds to sampling the upper bound curve at the midpoints $\frac{\bar{V}_{m,i-1}(t) + \bar{V}_{m,i}(t)}{2}$. This approach still slightly overestimates liquidity costs, which we consider preferable to underestimation (see the black curve *middle regression* in Figure 3).

In the remainder of the paper, we adopt sampling scheme (iii).

To support the parameterizations of $A_{m,\pm}(t)$ and $B_{m,\pm}(t)$, we compute at each time $0 \leq t \leq T_m$ the estimators $\hat{A}_{m,\pm}(t)$ and $\hat{B}_{m,\pm}(t)$ defined as the solutions to

$$(7) \quad \begin{aligned} & \operatorname{argmin} \\ & A_{m,+}(t) \geq 0, \\ & B_{m,+}(t) \geq 0 \end{aligned} \sum_{i>0} \left(L_m \left(t, \frac{\bar{V}_{m,i-1}(t) + \bar{V}_{m,i}(t)}{2} \right) - p_{m,i}(t) \right)^2 \mathbf{1}_{|\bar{V}_{m,i}(t)| \leq K}$$

and

$$(8) \quad \begin{aligned} & \operatorname{argmin} \\ & A_{m,-}(t) \geq 0, \\ & B_{m,-}(t) \geq 0 \end{aligned} \sum_{i<0} \left(L_m \left(t, \frac{\bar{V}_{m,i}(t) + \bar{V}_{m,i+1}(t)}{2} \right) - p_{m,i}(t) \right)^2 \mathbf{1}_{|\bar{V}_{m,i}(t)| \leq K},$$

where $p_{m,i}(t)$ is defined in (6). Figure 4 displays 10-minute rolling averages across trading days of $\hat{A}_{m,\pm}(t)$ and $\hat{B}_{m,\pm}(t)$, computed at each trade time using (7)–(8). The bid-ask spread for maturity

T_m at time $0 \leq t \leq T_m$ is given by

$$\lim_{x \rightarrow 0^+} L_m(t, x) - \lim_{x \rightarrow 0^-} L_m(t, x) = B_{m,+}(t) + B_{m,-}(t).$$

It decreases exponentially as time to maturity decreases, consistently with the findings of Balardy [4]. The slopes of $A_{m,\pm}(t)$ also decline as maturity approaches, indicating increasing liquidity. Using the 10-minute averages, we then perform least-squares regressions of the empirical estimates $\hat{A}_{m,\pm}(t)$ and $\hat{B}_{m,\pm}(t)$ against their theoretical counterparts given in (4) and (5). The estimated parameters are reported in Tables 1 and 2. These values may be useful for practitioners seeking to replicate our price impact simulations. The estimates are consistent with market developments: liquidity increased markedly at the beginning of 2022 (following the war in Ukraine and the shut-down of several French nuclear plants in late 2021), before slightly declining in 2023. This pattern is reflected in the dynamics of the spread parameters $\alpha_{B_{m,\pm}}$ and $\beta_{B_{m,\pm}}$ and of the slope parameters $\alpha_{A_{m,\pm}}$ and $\beta_{A_{m,\pm}}$. Regression results for January 2021 in France are shown in Figure 4.

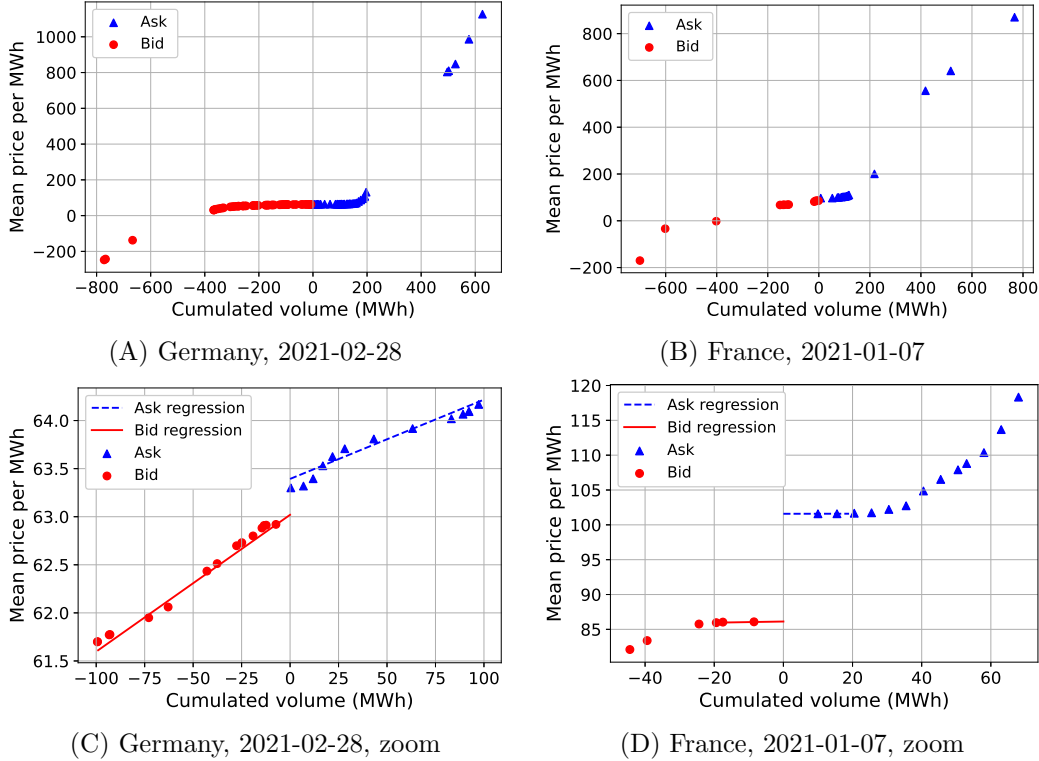


FIGURE 2. Example of empirical liquidity curves represented by the points $(\bar{V}_{m,i}(t), p_{m,i}(t) + \frac{F_{m,-1}(t) + F_{m,1}(t)}{2})$ for $i \neq 0$, with $\bar{V}_{m,i}(t)$ the cumulated volume and the weighted average price for number i on German and French market for maturity 18h, $t = 3$ hours before maturity, together with a linear regression on the bid side and a linear regression on the ask side for cumulated volumes such that $|\bar{V}_{m,i}(t)| \leq 100$ MWh on German market and $|\bar{V}_{m,i}(t)| \leq 20$ MWh on French market.

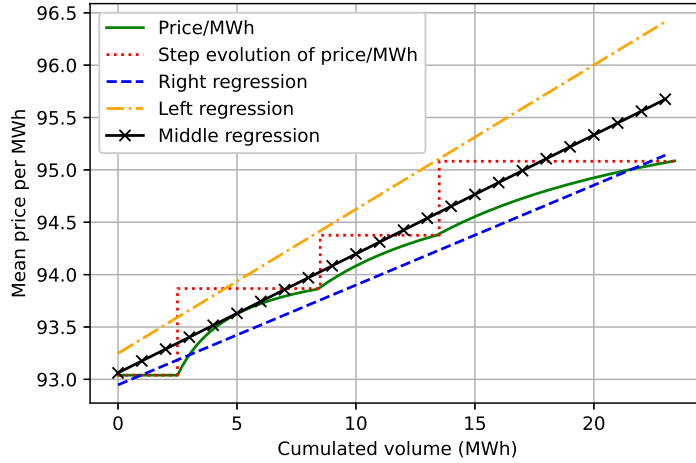


FIGURE 3. Different representations of the liquidity cost per unit volume on the ask side. The green solid curve shows the empirical liquidity cost curve. The red dashed curve represents its piecewise constant upper bound. The black line with x markers corresponds to the linear regression based on midpoint sampling of the piecewise constant upper bound, $\frac{\bar{V}_{m,i-1}(t) + \bar{V}_{m,i}(t)}{2}$, $i \geq 1$. The orange dashed curve is the linear regression based on sampling the piecewise constant upper bound at $\bar{V}_{m,i}(t)$, $i \geq 1$, while the blue dashed curve is the linear regression based on sampling the empirical liquidity cost curve at $\bar{V}_{m,i}(t)$, $i \geq 1$.

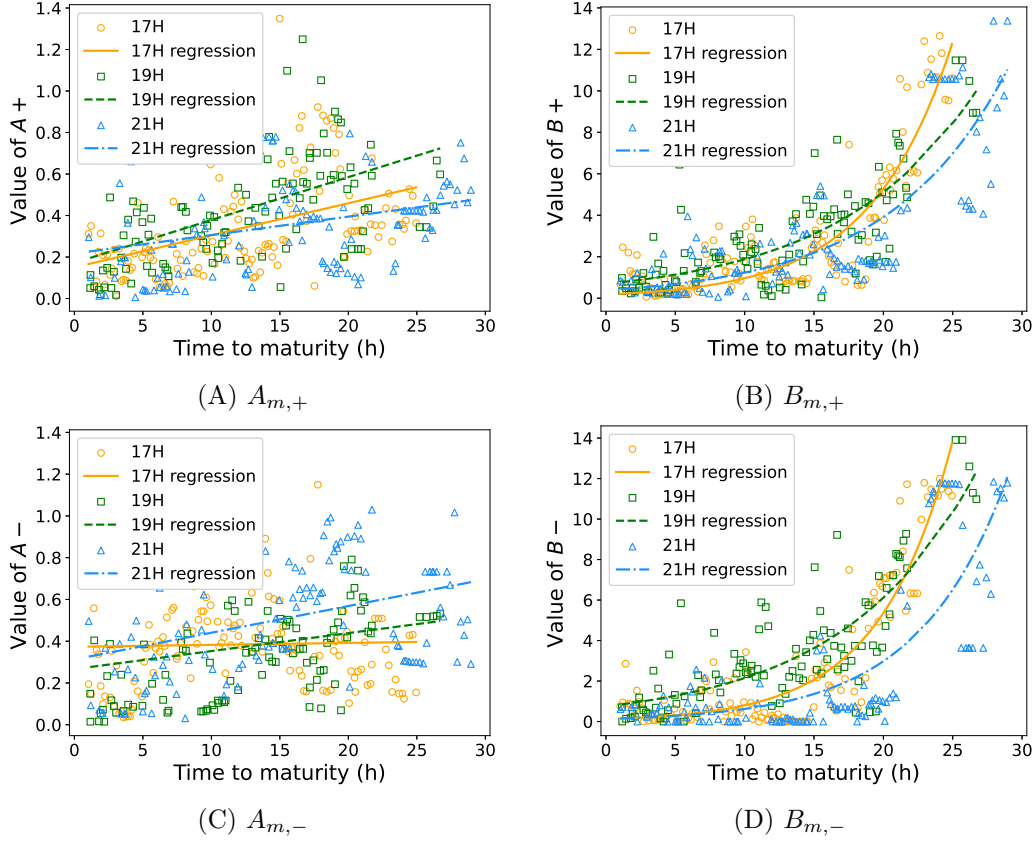


FIGURE 4. Temporal evolution of the estimated parameters $\hat{A}_{m,\pm}$ and $\hat{B}_{m,\pm}$ obtained from (7)–(8), computed at each order book update when at least five orders are present on each side, for different maturities T_m in the French market (January 2021). Each point corresponds to the 10-minute average parameter value for a given maturity (averaged across trading days). The solid lines represent the least-squares fit of the parametric models (4) and (5).

Year	$\alpha_{A_{m,+}} T_m$	$\beta_{A_{m,+}}$	$\alpha_{B_{m,+}} T_m$	$\beta_{B_{m,+}}$	$\alpha_{A_{m,-}} T_m$	$\beta_{A_{m,-}}$	$\alpha_{B_{m,-}} T_m$	$\beta_{B_{m,-}}$
2021	0.1751	0.0122	2.6968	-1.8208	0.0859	0.0240	3.6898	-2.2508
2022	1.1047	0.0444	45.1306	-42.5020	0.4828	0.0922	33.3084	-30.8538
2023	1.2883	0.1069	11.4713	-9.0995	0.4282	0.1792	16.3157	-13.0680

TABLE 1. Average parameters over the different maturities for Germany in January 2021, 2022 and 2023, calibrated over full trading sessions with normalised time from (7) and (8). For the α parameters, we multiply them by the duration of the trading session (which is equivalent to rescaling the time by T_m) to give them the same order of magnitude before averaging them. For example, to apply these parameters specifically to the 8-hour (8H) product, the parameter α given in this table should be divided by a factor of $8 + 9 = 17$. Here the extra 9 hours represent the time between the opening of the session and midnight.

Year	$\alpha_{A_{m,+}} T_m$	$\beta_{A_{m,+}}$	$\alpha_{B_{m,+}} T_m$	$\beta_{B_{m,+}}$	$\alpha_{A_{m,-}} T_m$	$\beta_{A_{m,-}}$	$\alpha_{B_{m,-}} T_m$	$\beta_{B_{m,-}}$
2021	0.1854	0.2517	3.2813	-0.6146	0.1468	0.2746	3.5512	-0.7842
2022	1.8613	0.7615	5.7148	-1.3478	1.5962	0.6560	3.3275	0.4182
2023	0.3440	0.6388	7.8779	-3.0430	0.6829	0.4090	7.6798	-2.8904

TABLE 2. Same as Table 1, for France.

To estimate the model within the battery valuation framework of Section 3, we consider trading days $d = 1, \dots, D$ where D denotes the number of distinct trading sessions used for estimation. Let $(\tau_{m,i}^d)_{i \geq 1}$ be the order book update times for day d and maturity T_m . The parameters $\alpha_{A_{\pm,m}}$, $\beta_{A_{\pm,m}}$ and $\beta_{B_{\pm,m}}$ are obtained as the solutions to

$$(9) \quad \begin{aligned} & \underset{\substack{\alpha_{A_{m,+}} \geq 0, \beta_{A_{m,+}} \geq 0, \\ \alpha_{B_{m,+}} \geq 0, \beta_{B_{m,+}} \geq 0}}{\text{argmin}} \sum_{\substack{d=1, \dots, D, \\ \tau_{m,k}^d, i > 0}} \mathbf{1}_{|\bar{V}_{m,i}^d(\tau_{m,k}^d)| \leq K} \left(L_m \left(\tau_{m,k}^d, \frac{\bar{V}_{m,i-1}^d(\tau_{m,k}^d) + \bar{V}_{m,i}^d(\tau_{m,k}^d)}{2} \right) \right. \\ & \quad \left. - p_{m,i}^d(\tau_{m,k}^d) \right)^2. \end{aligned}$$

and

$$(10) \quad \begin{aligned} & \underset{\substack{\alpha_{A_{m,-}} \geq 0, \beta_{A_{m,-}} \geq 0, \\ \alpha_{B_{m,-}} \geq 0, \beta_{B_{m,-}} \geq 0}}{\text{argmin}} \sum_{\substack{d=1, \dots, D, \\ \tau_{m,k}^d, i < 0}} \mathbf{1}_{|\bar{V}_{m,i}^d(\tau_{m,k}^d)| \leq K} \left(L_m \left(\tau_{m,k}^d, \frac{\bar{V}_{m,i}^d(\tau_{m,k}^d) + \bar{V}_{m,i+1}^d(\tau_{m,k}^d)}{2} \right) \right. \\ & \quad \left. - p_{m,i}^d(\tau_{m,k}^d) \right)^2. \end{aligned}$$

Here, $\bar{V}_{m,i}^d(t)$ denotes the cumulative volume at time $0 \leq t \leq T_m$, on day d , at level i of the order book, and $p_{m,i}^d(t)$ is the weighted average price defined in (6) for day d . To ensure consistency

with financial intuition and empirical evidence, we impose the constraints

$$\alpha_{A_{m,\pm}}, \beta_{A_{m,\pm}}, \alpha_{B_{m,\pm}} \geq 0$$

so that price impacts have the correct sign and decrease as time to maturity shortens. In the battery valuation framework, trading decisions are made one or two hours before delivery. Accordingly, we set the time to maturity to $T_m - t = 1$ hour for the one-hour-ahead decisions and to $T_m - t = 2$ hours for the two-hour-ahead decisions. To improve estimation accuracy, we restrict the dataset to specific time windows. For the two-hour-ahead strategy, we use observations from $T_m - t = 2.5$ to $T_m - t = 1.5$ hours. For the one-hour-ahead strategy, we use observations from $T_m - t = 1.5$ to $T_m - t = 1$ hour (data between $T_m - t = 1$ and $T_m - t = 0.5$ hours are excluded, see Section 1.3 for the justification).

2.2. Mid-price modeling. In this section, we use the model of Deschatre and Warin [14] for modeling mid-prices and recall some results from [14]. The model is constructed from three-dimensional Poisson measures, but for simplicity we give the construction based on compound Poisson processes given in [14, Corollary 3.1]. Fix μ , μ_c , and $\kappa > 0$. On a probability space $(\Omega, \mathcal{F}, \mathbb{P})$, let $P_1^+, P_1^-, \dots, P_M^+, P_M^-, P_1^{c,+}, P_1^{c,-}, \dots, P_M^{c,+}, P_M^{c,-}$ be $4M$ independent compound Poisson processes with intensities at time s given by

$$\begin{aligned} & - \mu e^{-\kappa(T_m-s)} \text{ for } P_m^+ \text{ and } P_m^-, m \geq 1, \\ & - \mu_c e^{-\kappa(T_M-s)} \text{ for } P_M^{c,+} \text{ and } P_M^{c,-}, \\ & - \mu_c e^{-\kappa(T_m-s)} - \mu_c e^{-\kappa(T_{m+1}-s)} \text{ for } P_m^{c,+} \text{ and } P_m^{c,-}, m = 1, \dots, M-1, \end{aligned}$$

and jump distribution $\nu(dy)$ on a measurable space (K, \mathcal{K}) , $K \subset \mathbb{R}_+$, with $\nu(\{0\}) = 0$ and $\int_K y^2 \nu(dy) < \infty$. The filtration $(\mathcal{F}_t)_t$ considered in the following is the natural filtration of all these compound Poisson processes.

If $f_{m,0}$ denotes the initial price for maturity T_m , then the price at time t given by $(x \wedge y)$ is the notation for the minimum of x and y)

$$(11) \quad f_{m,t} = f_{m,0} + f_{m,t \wedge T_m}^+ - f_{m,t \wedge T_m}^-,$$

with

$$(12) \quad f_{m,t}^h = P_{m,t}^h + \sum_{j=m}^M P_{j,t}^{c,h}$$

for $h = +, -, m = 1, \dots, M$ and $0 \leq t \leq T$. $f_{m,t}^+$ is the sum of the positive jumps of the process for maturity m up to time t , $f_{m,t}^-$ is the sum of the negative ones. Each of these processes is the sum of a compound Poisson process $P_{m,t \wedge T_m}^h$ specific to the maturity m and a jump process $\sum_{j=m}^M P_{j,t \wedge T_m}^{c,h}$ that correlates the different maturities. The last term represents a common shock occurring in the market and affecting all maturities (e.g. power plant failure, increase in temperature forecast): a jump occurring in $P_k^{c,h}$ affects the prices with maturity T_1, \dots, T_k simultaneously and in the same direction. Common shock modeling is a standard way to create correlation between Poisson processes [30, 27]. The price process $(f_m)_{m \in \{1, \dots, M\}}$ is a square-integrable $(\mathcal{F}_t)_t$ martingale from [14, Proposition 1].

If we look at $f_{m,t}^h$, it is easy to see that it is a compound Poisson process with jump distribution ν and intensity

$$\mu e^{-\kappa(T_m-t)} + \sum_{j=m}^{M-1} (\mu_c e^{-\kappa(T_j-t)} - \mu_c e^{-\kappa(T_{j+1}-t)}) + \mu_c e^{-\kappa(T_M-t)} = (\mu + \mu_c) e^{-\kappa(T_m-t)}.$$

The intensity of the price changes for the maturity m is the intensity of the jumps of $f_{m,t}^+ + f_{m,t}^-$, i.e.

$$(13) \quad 2(\mu + \mu_c)e^{-\kappa(T_m-s)}$$

and increases as time approaches maturity, which is consistent with the empirical findings on mid-prices in [13, 5]. A proxy for the integrated volatility of the price process for maturity m up to time t , obtained from the expectation of the quadratic variation, is $\int_0^{t \wedge T_m} \sigma_s^2 ds$ with

$$(14) \quad \sigma_{m,t}^2 = 2 \int_K y^2 \nu(dy) (\mu + \mu_c) e^{-\kappa(T_m-t)},$$

see [14, Proposition 3] and the discussion below. The volatility parameter increases as time approaches maturity, as does the intensity of price changes: this is the so-called Samuelson effect and is consistent with the mid-price data, see [13].

Similarly, a proxy for the correlation can be computed from the quadratic covariation. For $k \neq l$, the correlation between f_k and f_l does not depend on t and, for $t \leq \min(T_k, T_l)$, is given by

$$(15) \quad \rho_{lk} = \frac{\mu_c}{\mu + \mu_c} e^{-\frac{\kappa}{2}|T_l - T_k|}.$$

The correlation decreases with the distance between the two maturities: this is called the Samuelson correlation effect. This effect has been recently identified empirically for transaction prices in [14, 22]. It is also observed for the mid-prices in France and Germany, see Figure 5.

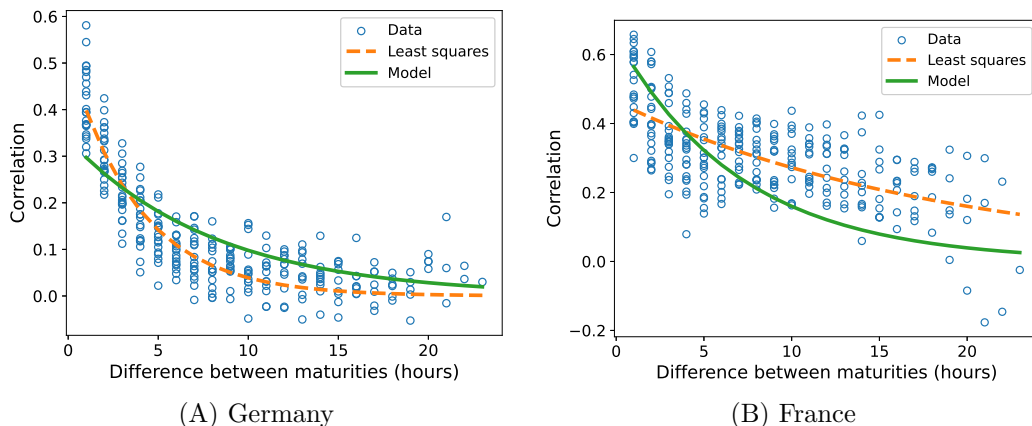


FIGURE 5. , estimated from the empirical quadratic covariation with a 30-minute sampling interval (blue dots), for German (left) and French (right) mid-prices in January 2021. The green line shows the model correlation computed from Equation (15). The dashed orange line shows a least-squares fit of κ and a to match the empirical correlation curve (blue) with the function $x \mapsto a \exp(-\frac{\kappa}{2}x)$.

This model requires only three parameters in addition to the law of jumps:

- (i) $\kappa > 0$ controls the rates at which the intensity of mid-price changes given by Equation (13) and the volatility given by Equation (14) increase. $\kappa/2$ is also the rate at which the correlation between two maturities given by Equation (15) decreases as the distance between maturities increases;

- (ii) $\mu > 0$ is a measure of the intensity of mid-price movements occurring independently at each maturity;
- (iii) $\mu_c > 0$ is a measure of the intensity of common shocks that affect several maturities simultaneously.

Finally, note that a diffusion approximation of this model (obtained with large μ and μ_c) is

$$\left(\int_0^{t \wedge T_m} \sigma_{m,s} dW_{m,s} \right)_{m=1, \dots, M}, \quad t \in [0, T]$$

where $W = (W_1, \dots, W_M)^\top$ is a multivariate Brownian motion with correlation matrix ρ_{lk} given by Equation (15) and $\sigma_{m,t}^2$ is defined in Equation (14), see [14, Proposition 6].

The estimation procedure is a moment-based method, with κ estimated from the intensity of mid-price moves, and μ and μ_c estimated from empirical quadratic variations and covariations, using a time step Δ large enough to remove microstructure noise; we set $\Delta = 30$ minutes. Note also that we treat returns whose absolute value exceeds five times the standard deviation of all non-zero returns over the estimation period as outliers and remove them as in [14]. We report the estimated parameters for the three estimation periods January 2021, January 2022, and January 2023 for Germany and France respectively in Table 3 and Table 4, as well as empirical estimators of the first two moments of the jump size distribution. The empirical jump size distribution is used in simulations. The intensities μ and μ_c are much higher for Germany, implying a higher frequency of mid-price movements. Jump sizes are significantly larger in the French market, indicating a sparser order book. This is consistent with the German market being more liquid than the French market. The high values of the jump sizes make the proxy parameter for the integrated variance $\sigma = \lim_{T_m \rightarrow \infty} \sqrt{\int_0^{T_m} \sigma_{m,s}^2 ds}$ higher for France than for Germany. We also notice an increase in this proxy parameter in 2022, which corresponds to a period of heightened volatility following the outbreak of the war in Ukraine (which affected gas prices) and some nuclear plant shutdowns at the end of 2021 in France. The correlation parameter ρ_1 between two consecutive products is of the same order of magnitude across the two countries and the different years Figure 5 shows that the correlation between two consecutive maturities is underestimated for the German data, and for the French data when maturities T_m and T_k satisfy $|T_k - T_m| \geq 6$ hours. One way to improve the fit of the empirical correlation curve would be to estimate the parameter κ directly using a least-squares procedure applied to the correlation curves shown in Figure 5. However, this may reduce the quality of the intensity curve fit. An alternative approach would be to use a criterion that incorporates both empirical intensities and correlations, achieving a better compromise between the two.

Year	κ	μ	μ_c	$\int_K y\nu(dy)$	$\int_K y^2\nu(dy)$	σ	ρ_1
2021	0.25	109.45	55.45	0.09	0.04	7.60	0.26
2022	0.28	195.12	214.02	0.22	0.58	41.51	0.40
2023	0.23	181.09	172.83	0.13	0.21	25.20	0.39

TABLE 3. Estimated parameters of model (11)-(12) for German mid-prices in January of 2021, 2022, and 2023. Units of κ , μ and μ_c are inverse hours (h^{-1}). $\sigma = \lim_{T_m \rightarrow \infty} \sqrt{\int_0^{T_m} \sigma_{m,s}^2 ds}$ is a proxy for the integrated volatility (see Equation (14)). ρ_1 denotes the correlation between two consecutive products (ρ_{ij} in Equation (15) for $|i - j| = 1$).

Year	κ	μ	μ_c	$\int_K y\nu(dy)$	$\int_K y^2\nu(dy)$	σ	ρ_1
2021	0.28	11.50	21.33	0.32	1.28	17.32	0.49
2022	0.36	31.90	34.23	0.83	6.75	49.55	0.36
2023	0.19	20.78	42.19	0.35	3.11	45.77	0.56

TABLE 4. Same as Table 3, for France.

3. NUMERICAL RESULTS

3.1. Optimizing position on one product. In [14] it has been shown that the proposed model is a good candidate for valuing a battery in the intraday market and gives a good strategy that outperforms in backtesting deterministic classical strategies based on the hourly spot values taken as a perfect forecast of the intraday prices of the same delivery periods. Without taking into account the liquidity of the market, the previous result is only valid when there are a small number of batteries in the market.

In this section, we show that accounting for market liquidity is crucial for accurately valuing batteries, particularly when many batteries are present in the market. Moreover, since the market is imperfect, it is also relevant to decide which product to use to take decisions: if a decision concerns the management of the battery at a given hour H , the decision must be taken at the time $H - \Delta$, where Δ should be between 1 and a few hours, since the market is illiquid. Therefore at the date $H - \Delta$, we buy or sell a product with maturity H and it induces a command of filling or emptying the battery at date H . We consider the case of a 2h battery and the case of a 3h battery. A nh battery has the following characteristics:

- the capacity of the battery is n MWh;
- the injection and withdrawal capacities are 1MWh per hour.

The battery efficiency is assumed to be $\rho = 0.92$, so:

- putting E MWh into storage requires withdrawing $\frac{E}{\rho}$ MWh from the grid, so we buy the equivalent amount on the market;
- withdrawing E MWh from storage only adds ρE MWh to the grid, and is therefore equivalent to selling that amount on the market.

As in [14], we consider the intraday prices $f_{m,t}$ for the delivery period $[T_m, T_m + \theta]$ with $\theta = 1$ hour, with $T_1 = 0, \dots, T_{24} = 23$ (every hour of the day). Decisions are made every hour with a

delay of $\Delta = 1$ or 2 hours, so that the decision for hour T_m is based on the price $f_{m, T_m - \Delta}$ for each $m \in \{1, \dots, 24\}$. The battery is managed assuming zero inventory at $T_1 = 0$ hour each day. The objective function is to maximize the expected profit at $T_0 = 15$ h on the day before management, which is the opening of the intraday market for the maturities under consideration. Taking into account the liquidity model, the purchase of a volume V (positively counted if purchase) at date $T_m - \Delta$ for delivery at date T_m , costs a price P per unit of volume:

$$P(m, \Delta, V) = f_{m, T_m - \Delta} + [A_{m,-}(T_m - \Delta)V - B_{m,-}(T_m - \Delta)]\mathbf{1}_{\{V < 0\}} + [A_{m,+}(T_m - \Delta)V + B_{m,+}(T_m - \Delta)]\mathbf{1}_{\{V > 0\}}.$$

The non-anticipative control taken at the time $T_i - \Delta$ belonging to $\mathcal{F}_{T_i - \Delta} = \{f_{m,s} | s \leq T_i - \Delta, m = 1, \dots, 24\}$ is noted C_i (a positive C_i corresponds to an injection) and we note $\tilde{C} = (C_1, \dots, C_{24})$. For a number of batteries \hat{N} present, and since all batteries are identical, the control is the same for each battery and the value function of a single battery is obtained by optimizing J :

$$(16) \quad J(\tilde{C}) = -\mathbb{E}\left[\sum_{i=1}^{24} C_i \left(\frac{1}{\rho} \mathbf{1}_{C_i \geq 0} + \rho \mathbf{1}_{C_i \leq 0}\right) P(i, \Delta, \hat{N} C_i \left(\frac{1}{\rho} \mathbf{1}_{C_i \geq 0} + \rho \mathbf{1}_{C_i \leq 0}\right)) \middle| \mathcal{F}_{T_0}\right]$$

with the constraints for $i = 1, \dots, 24$:

$$\begin{aligned} 0 &\leq \sum_{j=1}^i C_j \leq \bar{C}, \\ -\underline{C} &\leq C_i \leq \underline{C}. \end{aligned}$$

In our case, $\bar{C} = n$ and $\underline{C} = 1$.

Remark 1. Equation (16) gives the value of a single battery in a fleet of \hat{N} batteries. The number of batteries in the fleet only affects the price term P in the equation.

Remark 2. Battery managers are concerned with the number of cycles performed per year, which is limited for warranty reasons. This limitation creates a coupling between days and poses an intractable problem for our method. This constraint is very restrictive when operating on the reserve market (ancillary services). On the intraday market, in a previous study with the same price model but not taking liquidity into account (see remark 7 in [14]) we calculated the number of cycles per day a posteriori. We found that this number is around 1.5 cycles per day on the French market and about 1.6 on the German market for a 3-hour battery, and slightly higher for a 2-hour battery. In practice, batteries used in France by the operator EDF have a limit of 1.5 cycles per day, and this limit tends to be higher for newer technologies. Moreover, adding liquidity constraints diminishes the number of cycles achieved. This justifies not considering the cycle constraint in our model.

In order to compute the conditional expectation with respect to all available information, we must regress the value function while taking all the available products into account. In Tables 4 and 5 of [14], we studied the influence of the number of products on the valuation and showed that using $p = 4, 5$, or 6 products with the shortest maturities $(f_{m+\Delta+i, T_m})_{i=0, p-1}$ yields the same results. Furthermore, in one case, we computed a reference valuation using all products and the machine-learning approach developed in [32]; it produced the same result, but at a much higher computational cost.

Therefore we keep only the information on 4 products of the shortest maturity using regressions with local adaptive linear bases from [8] in the StOpt library [18]: 500,000 Monte Carlo price

trajectories and 4 meshes in each dimension for $p \leq 4$, and one mesh per dimension beyond 4, giving us a total of $4^{p \wedge 4}$ meshes, are used to estimate conditional expectations optimizing (16). Moreover, due to the impact model, the problem (16) is no longer linear: the control is no longer bang-bang, and using dynamic programming it is necessary to discretize the stocks and commands finely (see [31]). In our test, all stocks and commands are discretized with a step of 0.1 MWh.

To use our model on a day D on a given market with a given Δ , we estimate the price model and the liquidity parameters using the last 28 days of data and parameters are updated every Monday. For each day D of the year, different stochastic optimizations are obtained:

- a first (Stochastic no depth model) solves (16) with the parameters set for the market under study on the current day, but without price impact, thus replacing $P(m, \Delta, \hat{N}C_i)$ by $f_{i, T_i - \Delta}$, giving an optimal intraday storage management strategy for the model used, assuming no price impact.
- a second (Stochastic depth model) solves (16) taking into account the impact model for a given number of batteries \hat{N} placed in the market, giving an optimal strategy for the model used assuming price impact and \hat{N} given.

These strategies can be compared to a ‘‘spot control’’ optimization strategy with or without price impact : in these strategies, the control is calculated from the spot prices $\{f_{i, T_0}\}_{i=1, \dots, 24}$ at T_0 . The optimal control $\tilde{D} = (D_1, \dots, D_{24})$ is obtained by maximising the following problem:

$$(17) \quad \hat{J}(\tilde{D}) = - \sum_{i=1}^{24} D_i \left(\frac{1}{\rho} 1_{D_i \geq 0} + \rho 1_{D_i \leq 0} \right) \hat{P}(i, \Delta, \hat{N} D_i \left(\frac{1}{\rho} 1_{D_i \geq 0} + \rho 1_{D_i \leq 0} \right)),$$

where

$$\hat{P}(m, \Delta, V) = f_{m, T_0} - [A_{m, -}(T_m - \Delta)V - B_{m, -}(T_m - \Delta)] \mathbf{1}_{\{V < 0\}} + [A_{m, +}(T_m - \Delta)V + B_{m, +}(T_m - \Delta)] \mathbf{1}_{\{V > 0\}}$$

considering the price impact, or $\hat{P}(m, V) = f_{m, T_0}$ if no price impact is considered. Equation (17) is solved under the constraints for $i = 1, \dots, 24$

$$\begin{aligned} 0 &\leq \sum_{j=1}^i D_j \leq \bar{C}, \\ -\underline{C} &\leq D_i \leq \underline{C}. \end{aligned}$$

So for the same day \hat{D} , two deterministic optimizations are achieved:

- The first (Deterministic no depth model) solves (17) without price impact, giving a first deterministic strategy independent of the number of batteries \hat{N} .
- The second (Deterministic depth model) solves (17) with price impact giving a deterministic strategy depending on \hat{N} .

The four strategies calculated (2 stochastic and 2 deterministic) for the given day \hat{D} can be tested in a back test using the available order book. Then, at each hour h of the day \hat{D} , the calculated strategies give us the volume of the product of maturity $h + \Delta$ to buy or sell and using the order book we get the exact cost or gain associated to our control. Therefore, for a given \hat{D} we get a profit associated to each strategy for a given \hat{N} and we can get for each year the actual profit that we could have obtained.

The results in Table 5 and Table 6 for the year 2021 indicate that initiating positions one hour before delivery is suboptimal. This is primarily because the XBID market closes one hour prior

to delivery, prompting traders to finalize their trades just before the closure. Consequently, a gradual decrease in liquidity is observed between 1.5 hours and 1 hour before maturity. This trend highlights the advantage of setting $\Delta = 2$, which leads to improved outcomes. Moreover, on both markets, the results with either a $2h$ or a $3h$ battery behave in the same way in 2021. In the years 2022 and 2023 we only provide in the Appendix A results for a $2h$ battery with $\Delta = 2$ hours in Table 9 and Table 10 respectively for France and Germany. The liquidity in France is rather low and even with a single battery, there is a small gain when taking into account the price impact as shown on Table 5. Going up to 20 batteries, as the price impact model has been fitted with a window depth of 20 MW, not taking into account the market impact can lead to heavy losses: we expect the profit with N batteries to be higher than the profit with M batteries if $M < N$: this is clearly not the case if we don't take into account the price impact in 2021. On the more liquid German market, the price impact model is fitted with a depth of 100 MW in Table 6. As expected for a single battery, the price impact model does not improve backtesting profits. Up to 20 batteries, the price impact model does not bring much more profit. In 2021, even with 50 batteries, the gains are small.

n	Δ	\hat{N} Model	1		10		20	
			Depth	No depth	Depth	No depth	Depth	No depth
2	1	Det.	21264	18657	11737	5718	-590	-17280
		Sto.	25965	23994	18446	9353	10954	-14248
	2	Det.	32152	31919	26772	24954	17579	13185
		Sto.	33914	33699	29757	26263	22504	11872
3	2	Det.	42612	41961	34287	31472	21318	13902
		Sto.	45397	44982	38305	35509	27901	17076

TABLE 5. Backtest gains (euros per battery) for the optimization of \hat{N} nh batteries for the year 2021 on the French market, for the different models. The market position is taken Δ hours before maturity. Det. is for Deterministic and Sto. for Stochastic.

n	Δ	\hat{N} Model	1		20		50		100	
			Depth	No depth	Depth	No depth	Depth	No depth	Depth	No depth
2	1	Det.	32178	32060	27672	26287	11649	5353	-24272	-84059
		Sto.	44727	44720	40535	39439	32318	23416	18481	-38972
	2	Det.	35584	35536	34287	33626	29450	27492	12011	4495
		Sto.	45500	45585	43711	43658	39760	38000	31543	17689
3	2	Det.	48891	48854	47043	46113	38874	36695	14079	3713
		Sto.	61752	61791	59297	59152	53313	51204	37295	21108

TABLE 6. Backtest gains (euros per battery) for the optimization of \hat{N} nh batteries for the year 2021 on the German market, for the different models. The market position is taken Δ hours before maturity. Det. is for Deterministic and Sto. for Stochastic.

In Figure 6 and Figure 7, we show the total gain of a fleet of \hat{N} batteries achieved in the backtest in 2023. When the number of batteries is below 20 in France and 40 in Germany, the gain is visually almost linear with the number of batteries, taking market depth into account. For Germany, neglecting market depth leads to substantial losses when the number of batteries exceeds 60.

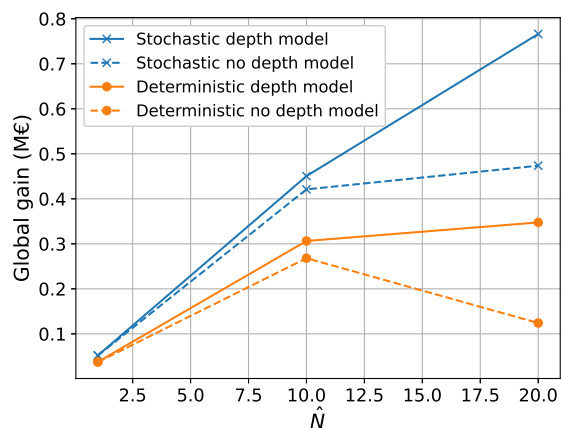


FIGURE 6. Global gain in millions of euros for a park of \hat{N} $2h$ batteries in France in 2023.

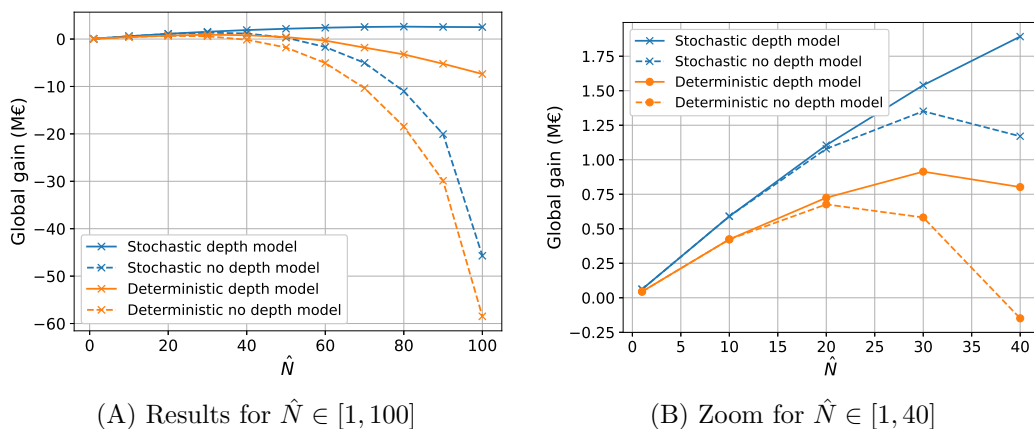


FIGURE 7. Global gain in millions of euros for a park of \hat{N} $2h$ batteries in Germany in 2023.

Accounting for liquidity is crucial, especially when the number of batteries is large: it enables much greater gains to be made and avoids losses. The use of a stochastic price model, as shown in [14], already improves the results even in the absence of liquidity modeling. Here, we show that incorporating liquidity further enhances performance.

3.2. Optimizing with commands on two products. In the previous section, we have studied the management of a battery taking a decision one ($\Delta = 1$) or two hours ($\Delta = 2$) before maturity. One may wonder if it is possible to take into account the dynamics of two products or more (given two or more maturities). Thus, for a given date t , we take positions for products with maturities $t + 2h$ and $t + 3h$: the real control for the battery at date t is given by the sum of the two positions taken at date $t - 2h$ and $t - 3h$. Since the price model used without price impact is a martingale, there is theoretically no advantage in trading two maturities simultaneously in the absence of market impact. The possibility to trade two products is only a way with our model to have more liquidity and splitting a volume traded across both hours may be beneficial. We can try to optimize the previous problem by making two decisions at each hour and backtesting our strategy. This problem is much harder to solve because it is an optimization problem with 2 stocks: the first stock corresponds to the position taken on the product with a maturity of 3 hours, while the second corresponds to the additional volume traded 2 hours before maturity. In Table 7, we optimize a storage on a day at the beginning of 2021 with the stochastic price model, taking into account the market impact on the French and German markets, and report the theoretical battery profit as a function of \hat{N} . As expected, the profit of trading the two products is higher than that of trading a single product, as it is a special case of the two products problem taking 0 volume trading product with a maturity of 3 hours.

Country	\hat{N}	Gain one product	Gain two products
France	1	129	153
	10	108	129
	20	91	111
Germany	1	113	120
	10	106	112
	20	100	107
	50	84	95

TABLE 7. Theoretical gain (euros per battery) for \hat{N} 2h battery with the model trading products $T_m + 2$, $T_m + 3$ (gain two products) versus trading only product $T_m + 2$ (gain one product) for France and Germany with parameters estimated on December 28, 2020..

Backtesting the two-products strategy for a full year is computationally too expensive. Therefore, we backtest it only for the first 50 days of 2021 with $\hat{N} = 1$ and give results in Table 8. The backtest of the two-product strategy results in a significant loss compared to the single-product case. The price model used and especially the correlation structure in it is not realistic enough to handle the two-products case.

Market	Gain one product	Gain two products
France	2170	487
Germany	2269	1620

TABLE 8. Backtest gains (euros per battery) for one $2h$ battery with the model trading products $T_m + 2$, $T_m + 3$ (gain two products) versus trading only product $T_m + 2$ (gain one product) for France and Germany on the first 50 days of 2021.

4. CONCLUSION

In this work, we have proposed a complete modeling framework for battery valuation during an intraday trading session addressed to practitioners that includes i) volatility and correlation modeling ii) liquidity costs modeling and iii) asset modeling and optimization. While it has already been shown in [14] that it is of particular importance to take volatility and correlation into account for battery valuation on intraday markets, we extend their work by including liquidity costs. With a simple deterministic model for liquidity, we show that we can improve the gains obtained by several batteries on a backtest exercise on the German and French markets. Furthermore, we show that not taking into account these liquidity costs while developing a trading strategy can induce substantial losses, especially when optimizing several batteries.

Future research includes

- (1) The improvement of the mid-price model by including the modeling of microstructure effects, see [14], for instance by using more sophisticated point processes such as Hawkes processes used in [13, 11]. An alternative approach would be to directly model the order book for the different maturities extending the work of [5], to have access both to the dynamics of the price and of the liquidity and to make liquidity stochastic as well, which is not the case in our model.
- (2) The joint optimization of a wind farm and a battery. The wind farm could reduce liquidity costs, while the battery could reduce imbalances. This would require the joint modeling of the price, the liquidity, and the wind production.
- (3) The joint optimization on several markets including spot and ancillary markets, as well as the handling of imbalance penalties. We could also add the integration of European intraday auction markets which are recent and may significantly affect intraday liquidity.

ACKNOWLEDGEMENTS

The authors acknowledge support from the FiME Lab (Institut Europlace de Finance). The authors are grateful to Félix Trieu for his valuable help with the data and to Pierre Gruet and the anonymous referee for their constructive comments.

DISCLOSURE STATEMENT

The authors report there are no competing interests to declare.

REFERENCES

- [1] René Aïd, Andrea Cosso, and Huyên Pham. Equilibrium price in intraday electricity markets. *Mathematical Finance*, 32(2):517–554, 2022.
- [2] René Aïd, Pierre Gruet, and Huyên Pham. An optimal trading problem in intraday electricity markets. *Mathematics and Financial Economics*, 10:49–85, 2016.

- [3] Achref Bachouch, Côme Huré, Nicolas Langrené, and Huyên Pham. Deep neural networks algorithms for stochastic control problems on finite horizon: numerical applications. Methodology and Computing in Applied Probability, 24(1):143–178, 2022.
- [4] Clara Balardy. An empirical analysis of the bid-ask spread in the continuous intraday trading of the german power market. The Energy Journal, 43(3), 2022.
- [5] Philippe Bergault and Enzo Cognéville. Simulating and analyzing a sparse order book: an application to intraday electricity markets. Quantitative Finance, 25(10):1599–1614, 2025.
- [6] Marcel Blais and Philip Protter. An analysis of the supply curve for liquidity risk through book data. International Journal of Theoretical and Applied Finance, 13(06):821–838, 2010.
- [7] Alexander Blasberg, Nikolaus Graf von Luckner, and Rüdiger Kiesel. Modeling the serial structure of the Hawkes process parameters for market order arrivals on the German intraday power market. In 2019 16th International Conference on the European Energy Market (EEM), pages 1–6. IEEE, 2019.
- [8] Bruno Bouchard and Xavier Warin. Monte-Carlo valuation of American options: facts and new algorithms to improve existing methods. In Numerical Methods in Finance: Bordeaux, June 2010, pages 215–255. Springer, 2012.
- [9] René Carmona and Michael Ludkovski. Valuation of energy storage: An optimal switching approach. Quantitative finance, 10(4):359–374, 2010.
- [10] Ümut Cetin, Robert Jarrow, Philip Protter, and Mitch Warachka. Pricing options in an extended black scholes economy with illiquidity: Theory and empirical evidence. The Review of Financial Studies, 19(2):493–529, 2006.
- [11] Konstantinos Chatziandreu and Sven Karbach. Optimal execution in intraday energy markets under hawkes processes with transient impact. Quantitative Finance, pages 1–27, 2026.
- [12] Jérôme Collet, Olivier Féron, and Peter Tankov. Optimal management of a wind power plant with storage capacity. In Renewable Energy: Forecasting and Risk Management: Paris, France, June 7-9, 2017 1, pages 229–246. Springer, 2018.
- [13] Thomas Deschatre and Pierre Gruet. Electricity intraday price modelling with marked Hawkes processes. Applied Mathematical Finance, pages 1–34, 2023.
- [14] Thomas Deschatre and Xavier Warin. A common shock model for multidimensional electricity intraday price modelling with application to battery valuation. Quantitative Finance, pages 1–20, 2024.
- [15] Benjamin Favetto. The european intraday electricity market: a modeling based on the hawkes process. Journal of Energy Markets, 2020.
- [16] Olivier Féron, Peter Tankov, and Laura Tinsi. Price formation and optimal trading in intraday electricity markets with a major player. Risks, 8(4):133, 2020.
- [17] Elisabeth Finhold, Till Heller, and Neele Leithäuser. On the potential of arbitrage trading on the german intraday power market. Journal of Energy Markets, 16(3), 2023.
- [18] Hugo Gevret, Nicolas Langrené, Jerome Lelong, Xavier Warin, and Aditya Maheshwari. STochastic OPTimization library in C++. 2018.
- [19] Silke Glas, Rüdiger Kiesel, Sven Kolkmann, Marcel Kremer, Nikolaus Graf von Luckner, Lars Ostmeier, Karsten Urban, and Christoph Weber. Intraday renewable electricity trading: Advanced modeling and numerical optimal control. Journal of Mathematics in Industry, 10:1–17, 2020.
- [20] Nikolaus Graf von Luckner and Rüdiger Kiesel. Modeling market order arrivals on the German intraday electricity market with the Hawkes process. Journal of Risk and Financial Management, 14(4), 2021.
- [21] Ria Grindel and Nikolaus Graf von Luckner. Forecasting of the id3 using limit order book data. Available at SSRN 4017248, 2022.
- [22] Simon Hirsch and Florian Ziel. Multivariate simulation-based forecasting for intraday power markets: Modeling cross-product price effects. Applied Stochastic Models in Business and Industry, 2024.
- [23] Eduardo Abi Jaber, Nathan De Carvalho, and Huyên Pham. Trading with propagators and constraints: applications to optimal execution and battery storage. arXiv preprint arXiv:2409.12098, 2024.
- [24] Daniel R Jiang and Warren B Powell. Optimal hour-ahead bidding in the real-time electricity market with battery storage using approximate dynamic programming. INFORMS Journal on Computing, 27(3):525–543, 2015.
- [25] Christopher Kath and Florian Ziel. Optimal order execution in intraday markets: Minimizing costs in trade trajectories. arXiv preprint arXiv:2009.07892, 2020.
- [26] Anke Kramer and Rüdiger Kiesel. Exogenous factors for order arrivals on the intraday electricity market. Energy Economics, 97:105186, 2021.
- [27] Filip Lindskog and Alexander J McNeil. Common Poisson shock models: applications to insurance and credit risk modelling. ASTIN Bulletin: The Journal of the IAA, 33(2):209–238, 2003.

- [28] R Machlev, N Zargari, NR Chowdhury, J Belikov, and Y Levron. A review of optimal control methods for energy storage systems-energy trading, energy balancing and electric vehicles. Journal of Energy Storage, 32:101787, 2020.
- [29] Pekka Malo and Teemu Pennanen. Reduced form modeling of limit order markets. Quantitative Finance, 12(7):1025–1036, 2012.
- [30] Miro R Powojowski, Diane Reynolds, and Hans JH Tuenter. Dependent events and operational risk. Algo Research Quarterly, 5(2):65–73, 2002.
- [31] Xavier Warin. Gas storage hedging. In Numerical methods in finance: Bordeaux, June 2010, pages 421–445. Springer, 2012.
- [32] Xavier Warin. Reservoir optimization and machine learning methods. EURO Journal on Computational Optimization, 11:100068, 2023.
- [33] Simon N Wood. Generalized additive models: an introduction with R. chapman and hall/CRC, 2017.

A. RESULTS FOR YEARS 2022 AND 2023

In this appendix we give for years 2022 and 2023 the different values obtained in back-test for a single battery of a park of \hat{N} batteries in Table 9 for the French market and Table 10 for the German market.

Year	\hat{N} Model	1		10		20	
		Depth	No depth	Depth	No depth	Depth	No depth
2022	Det.	68246	67263	59922	56031	42707	34959
	Sto.	76553	76570	68749	66480	60020	48130
2023	Det.	37785	37245	30626	26815	17378	6204
	Sto.	52122	51890	45052	42100	38311	23679

TABLE 9. Backtest gains (euros per battery) for the optimization of \hat{N} 2h batteries for the years 2022 and 2023 on the French market, for the different models. The market position is taken 2 hour before maturity. Det. is for Deterministic and Sto. for Stochastic.

Year	\hat{N} Model	1		20		50		100	
		Depth	N.D.	Depth	N.D.	Depth	N.D.	Depth	N.D.
2022	Det.	86591	86605	140591	80845	79625	56381	-18218	-101280
	Sto.	106882	106813	101778	101284	90521	79625	68123	-56460
2023	Det.	44812	44416	36246	33833	8164	-35606	-73747	-584819
	Sto.	61823	61824	55285	53964	43414	5852	25138	-457042

TABLE 10. Backtest gains (euros per battery) for the optimization of \hat{N} 2h batteries for the years 2022 and 2023 on the German market, for the different models. The market position is taken 2 hour before maturity. Det. is for Determinist, Sto. for Stochastic, and N.D. for No depth.